

FR-8387

**A New Class of Pulse Compression Codes
and Techniques**

**B.L. Lewis
F.F. Kretschmer**

March 26, 1980

Naval Research Laboratory

CONTENTS

INTRODUCTION	1
NEW CODES.....	1
NEW CODE UTILIZATION TECHNIQUES	2
EFFECT OF PRECOMPRESSION BANDWIDTH LIMITATIONS	5
EFFECT OF DOPPLER ON THE AUTOCORRELATION FUNCTIONS OF THE VARIOUS CODES UNWEIGHTED AND WEIGHTED	6
EFFECT OF PRECOMPRESSION BANDWIDTH LIMITATIONS ON SIGNAL-TO-NOISE RATIO	6
CONCLUSIONS	23
REFERENCES	23

**A NEW CLASS OF PULSE COMPRESSION
CODES AND TECHNIQUES**

INTRODUCTION

This report describes a new class of codes and digital pulse expander-compressor systems for use in radar and related fields. These new codes have complete symmetry about their midpoints which can be exploited to reduce the digital processing required in matched filter implementation. In addition, these new codes can be used to obtain higher peak to range-time sidelobe levels with less signal-to-noise ratio loss than any previous codes known to the authors.

NEW CODES

The new codes are called the Kretschmer-Lewis (KL) code and the Lewis-Kretschmer-Shelton (LKS) code. These codes are polyphase in nature like the Frank code [1]. In the Frank code, the phase of the i th code element in the j th code subgroup or frequency is

$$\phi_{i,j}^{\text{Frank}} = (2\pi/N)(i-1)(j-1), \quad (1)$$

where

$$i = 1, 2, 3, \dots, N,$$

and

$$j = 1, 2, 3, \dots, N.$$

In the Frank code, successive values of i are used for each value of j and the number of code elements formed is equal to N^2 . For example, the Frank code with $N = 3$ is

$$\begin{array}{ccccccccc} \phi_{1,1} & \phi_{2,1} & \phi_{3,1} & \phi_{1,2} & \phi_{2,2} & \phi_{3,2} & \phi_{1,3} & \phi_{2,3} & \phi_{3,3} \\ 0 & 0 & 0 & 0 & 2\pi/3 & 4\pi/3 & 0 & 4\pi/3 & 8\pi/3 \end{array}$$

Manuscript submitted January 2, 1980.

With the multiples of 2π phase ambiguities removed, the Frank code can be seen to be the conjugate steering phases of an N point discrete fourier transform (DFT) where the j th frequency coefficient is

$$F_j = \sum_{i=1}^N a_i e^{-j \frac{2\pi}{N} (i-1)(j-1)} \quad (2)$$

and where a_i is the i th input sample. This code produces the lowest autocorrelation function peak-sidelobes without amplitude weighting of any previously known code that is not limited in time-bandwidth product. For small time-bandwidth products ($N < 4$), the Frank code has the same peak-to-sidelobe level as the Barker code which has been called a perfect code. Unfortunately, the Barker code is limited to time-bandwidth products of 13 to 1 as opposed to the Frank code which can be derived for any desired time-bandwidth product.

The KL code, also consisting of N^2 elements where N is an odd integer, is represented mathematically as

$$\phi_{i,j} = (\pi/N)(i-1)(N+1-2j), \quad (3)$$

where i and j are integers ranging from 1 to N and have the same meaning as they do in the Frank code. The requirement that N be odd provides symmetry about a direct current (dc) term and eliminates a code group that would have π phase changes element to element. This is important in controlling autocorrelation function sidelobe levels and in making implementation much easier and less costly.

The KL code is similar to the Frank code in that it is derivable from a DFT. However, the code groups (frequencies) are taken in different order.

The LKS code also consists of N^2 elements where N is an even number. It is similar to the code derivable from a Butler matrix used to steer array antennas [2]. It can be represented mathematically as

$$\phi_{i,j} = \left[(\pi/N)(i-1) - (\pi/2) \frac{N-1}{N} \right] \left[N+1-2j \right], \quad (4)$$

where i and j are integers ranging from 1 to N . The requirement for N to be even in this code stems from the desire for low autocorrelation sidelobes. An N odd results in high autocorrelation sidelobes.

NEW CODE UTILIZATION TECHNIQUES

Cantrell and Lewis [3] suggested the first simplified digital pulse expander-compressor technique to be investigated at the Naval Research Laboratory (NRL). This suggestion involved replacing a bank of analog contiguous-band-pass-filters and differential analog

delay lines, such as those previously used in radar with a clocked digital DFT circuit and differential clocked shift register (SR) delays in each frequency output port. This logic is illustrated in Fig. 1 in a form developed by Lewis and Kretschmer on the basis of Cantrell's suggestion. The principle of operation is as follows:

The signal code to be transmitted (pulse expansion) is produced by inputting a single digital word sample (impulse) through switch S_1 into an N point DFT circuit or a fast fourier transform (FFT) circuit. In response to this single word sample input, N successive inphase I and quadrature Q words are clocked out of each frequency port F_1, F_2, \dots, F_N simultaneously. These words result from the input sample being clocked through the $i = 1, 2, \dots, N$ points of the input shift registers.

These I and Q words represent complex numbers that define both the phase and magnitude of the steering weights used in the DFT to produce its various digital filter banks using N successive time samples of input data. The N successive samples of the output of the F_N port are inputted to one input of a digital adder whose output passes through switch S_2 to a radar transmitter where each successive word defines the phase to be transmitted for a time interval equal to the clock period used in the DFT.

The output of the F_{N-1} port is simultaneously inputted to one input of a second digital adder whose output drives a chain of N shift registers operating at the clock rate used in the DFT. The output of this chain drives the second input of the adder driven by F_N . When the N pulses from F_N finally issue from S_2 , the N from F_{N-1} starts to issue contiguously from the N shift register delay line. A similar process is used with each output from a frequency port as shown in Fig. 1 to produce a stream of N^2 digital words lasting for N^2 times the clocking period in time. Thus the duration of the total coded transmitted pulse is N^2 times as long as the duration of one element in the code. When this total pulse exits from S_2 , S_1 and S_2 are thrown to their second position into a receive mode.

Pulse compression is achieved by coherently detecting echoes to baseband I and Q video, sampling these data at the DFT clock rate, converting these samples to digital words, conjugating the words (changing the sign of the Q words), and inputting these words into the inverse transform side of the DFT (Fig. 1).

Since F_N was the first code group or frequency to be transmitted, it will be the first back in any echo. Thus when the first N conjugated words of any echo index into the N points of the DFT, a word N times larger in magnitude than that of any single input word will issue from the F_N frequency port.

This F_N output will be connected to the input of an N shift register chain whose output is digitally added to the output from the F_{N-1} port. N sample periods after F_N indexed, F_{N-1} will index in the DFT points and produce an N times magnified output from the F_{N-1} port having the same phase as that from the F_N port. At this time, the N times magnified word out of F_N will issue from its shift register delay to add coherently with the magnified signal out of F_{N-1} . This process continues until the differentially delayed magnified words out of each matched port sum to a word magnified by N^2 when F_1 indexes into the DFT points. This N^2 magnified word is the desired compressed pulse and is outputted through switch S_2 to the user facility.

Prior to and after the compressed pulse issues from S_2 , mismatched responses (autocorrelation function sidelobes) will exit from S_2 starting with the first code element received and ending after the last code element received clears the DFT and the delay lines between F_1 output and S_2 .

Figure 2 is a computer-drawn plot of the autocorrelation function to be expected from the circuit of Fig. 1 with $N = 9$ with no doppler shift on the received signal. This function is identical to that of an 81-element Frank code. Note that the highest sidelobe is down from the peak by $\pi^2 N^2$. This is characteristic of the Frank code and is a factor of π^2 lower than other unweighted codes that provide unlimited pulse compression ratios [4,5].

Figure 3 illustrates the implementation of the KL code. Equations (1) and (3) identify the reordering of the frequencies transmitted. The same type of DFT is employed but N is restricted to odd integers so that the code can be rearranged symmetrically about the radar's carrier frequency (the zero frequency code group). This reordering halves the phase increments that are used in the high-frequency groups and removes ambiguities in these frequencies. At no time is a phase increment between code elements allowed to equal or exceed π radians as can be seen from Eq. (3). This will be shown to be important in pre-compression bandwidth limiting effects of IF amplifiers and implementation simplification.

Note that in the implementation in Fig. 3, the echo signal does not need to be conjugated and two sets of differential shift register delay lines are not required as in Fig. 1.

When F_3 is transmitted first, it is received first and, without conjugating, it will match the F_1 filter since this filter's weights are the conjugates of those in F_3 due to the code symmetry. Thus its match will be delayed properly by the same differential shift register delay line that was used to form the code.

Figure 4 depicts the autocorrelation function of a KL code with $N = 9$. Note that the highest sidelobes are down below the peak response by $\pi^2 N^2$ as in the Frank code. However, this new code offers an advantage not possessed by the Frank code.

When oversampled by 2 and processed as illustrated in Fig. 5, the autocorrelation function of the KL code changes to that illustrated in Fig. 6 while that of the Frank code remains essentially unchanged (Fig. 7). High frequency variations appear in Fig. 6 which are contained under the envelope of the nonoversampled code sidelobes. This implies that oversampling by 2 and digital filtering of the output by averaging two successive samples could be used to reduce the autocorrelation function sidelobes without significantly reducing the range resolution or the signal-to-noise ratio. This implication was found to be true as documented by Fig. 8. Note that the highest sidelobes in this example are reduced by 4.5 dB from the highest sidelobes of Fig. 6.

Since matched filters are linear networks, as long as the sampling rate is not changed in the process, the averaging filter can be placed ahead of the DFT filter networks as illustrated in Fig. 9. This permits an N point DFT operating at twice its normal sampling

rate to be used to process the $2N$ samples of data it operates on instead of requiring a $2N$ point network that would greatly increase the number of parts required.

Figure 10 illustrates the very small effect oversampling by 2 and averaging by 2 has on a conventional Frank code. Oversampling the KL by 2 and averaging by three (Fig. 11) significantly reduces the autocorrelation function sidelobes but also reduces the range resolution and signal-to-noise ratio.

Figure 12 portrays the implementation of the LKS code whose element phases are given by Eq. (4). This code differs from the Frank or the KL codes in that the code groups corresponding to frequencies are symmetrical about their centers as well as being symmetrical about the center of the complete code group. This code group symmetry makes it possible to input the conjugated received code for compression into the same input used to form the code. This eliminates the need for using two sets of I, Q shift registers as in Fig. 3 to obtain the N time samples that are used to drive the matrix filter networks. In other respects, this implementation works in a manner identical to that described for the KL code and can be oversampled and averaged (Fig. 13) with the same beneficial results (Figs. 14 and 15).

The symmetry of the KL and LKS codes permits another large saving to be made in hardware used for implementation. Conjugation of the phase shifted (weighted) samples that are summed to produce the filters for the frequencies below the carrier permits sample summing to be employed to generate the upper frequency filters. This halves the number of digital multipliers that must be used in the phase shifters in the filter banks.

The KL and LKS codes have another significant advantage over other codes, in that the overall code symmetry about their centers permit approximately a half matrix to be used to compress the code. The code to be transmitted can be read from a read-only memory and echoes can be compressed as illustrated in Fig. 16. This use of a half matrix greatly reduces the number of digital components required in the matrix.

In addition to oversampling and averaging, frequency-by-frequency amplitude weighting can be used to control sidelobes if desired on all of the codes discussed. Such weighting is applied at the output of the various frequency ports prior to summing in the differential delay lines and adders. Figure 17 illustrates the results of amplitude weighting the frequency ports of the compressor on receive with a cosine on a pedestal of 0.4.

EFFECT OF PRECOMPRESSION BANDWIDTH LIMITATIONS

The effect of a restricted bandwidth in the IF amplifiers and the I, Q detectors preceding analog to digital conversion and compression of the phase codes was investigated. The various codes to be compressed were oversampled by 5 to 1 and sliding window averaged by 5, 7, and 10 to simulate the precompression bandwidth limitation. The resultant waveform was then sampled every 5th sample and inputted to the compressor. To take time of arrival variations into account, the sliding window average was taken starting five, four, three, two, and one oversample periods ahead of the first received code element, and autocorrelation functions were developed for each case.

The results of this study revealed that precompression bandwidth limitations were similar to amplitude weighting the frequency output ports of the digital filters in the compressor when the symmetrical KL or LKS codes were employed and time-of-arrival variations were taken into consideration (Fig. 18). However, this was not the case when the normal (unsymmetrical) Frank code was processed (Fig. 19). In this case, the bandwidth limitation did not affect the dc term and had little effect on the highest frequency code subgroup since it is the conjugate of the frequency code subgroup closest to the dc term. As a consequence, precompression bandwidth limitation did not drop the far-out sidelobe caused by the dc term indexing into the highest frequency filter and vice versa.

EFFECT OF DOPPLER ON THE AUTOCORRELATION FUNCTIONS OF THE VARIOUS CODES UNWEIGHTED AND WEIGHTED

The first effect that appears with increasing doppler on echoes of frequency derived polyphase codes such as the Frank, KL or LKS is a progressive phase shift in the code subgroups obtained from the various frequency ports of the digital filter banks. This significant effect has not been noted in any literature known by the authors. A second effect only noticeable at high Doppler shifts is a change in the phase increments used from code element to code element in the definition of the different frequencies. The former effect causes the peak response to vary cyclically from zero dB to nearly - 4 dB and back with Doppler as illustrated in Fig. 20 without modifying the far-out sidelobe structure significantly. The minimums occur at every odd multiple of π phase shift across the uncompressed pulse due to Doppler which corresponds to odd multiples of half range cell range-Doppler-coupling. The latter effect modifies the far out sidelobes by making sampled Doppler-shifted high frequencies match low-frequency filters that use discrete phase weights (Fig. 21).

The cyclic loss and mainlobe broadening associated with the first Doppler effect can be controlled by oversampling and averaging or by amplitude weighting the frequency output ports in the compressor (Fig. 22). Such weighting also increases the mainlobe-to-sidelobe ratio which is desirable. However, it also reduces the obtainable signal-to-noise ratio out of the compressor by a small amount on the order of 1 dB.

At this point, however, it should be noted that the relatively small Doppler shifts that produce the first effect correspond to very high velocity targets at surveillance radar carrier frequencies. This important fact is illustrated in Fig. 20, which reveals that the first peak to minimum cycle spans a target velocity range from zero to Mach 5 at a carrier frequency of 1 GHz with a radar bandwidth of 2 MHz.

EFFECT OF PRECOMPRESSION BANDWIDTH LIMITATIONS ON SIGNAL-TO-NOISE RATIO

The phase codes discussed in this report have $(\sin x)/x$ spectrum envelopes (Figs. 23 and 24). Note that the LKS (and KL) code has a much more symmetrical spectrum than the Frank code due to its symmetry about the carrier.

The average loss of the peak values shown in Figs. 18 and 19 was computed to be approximately 2.3 dB for both the Frank and the LKS codes. Some of this loss can be attributed to the passband limitation, while the remaining loss represents the loss due to time-of-arrival variation or range cusping. The thermal noise contribution is the same for each code in Figs. 18 and 19 and is determined by the width of the passband. It is important to note, however, that the symmetrical KL or LKS code sidelobes drop more than the peak due to precompression bandwidth limitation while those of the Frank code do not drop at all. This results in much lower sidelobes in the new codes for the same signal-to-noise ratio loss due to the precompression bandwidth limitation.

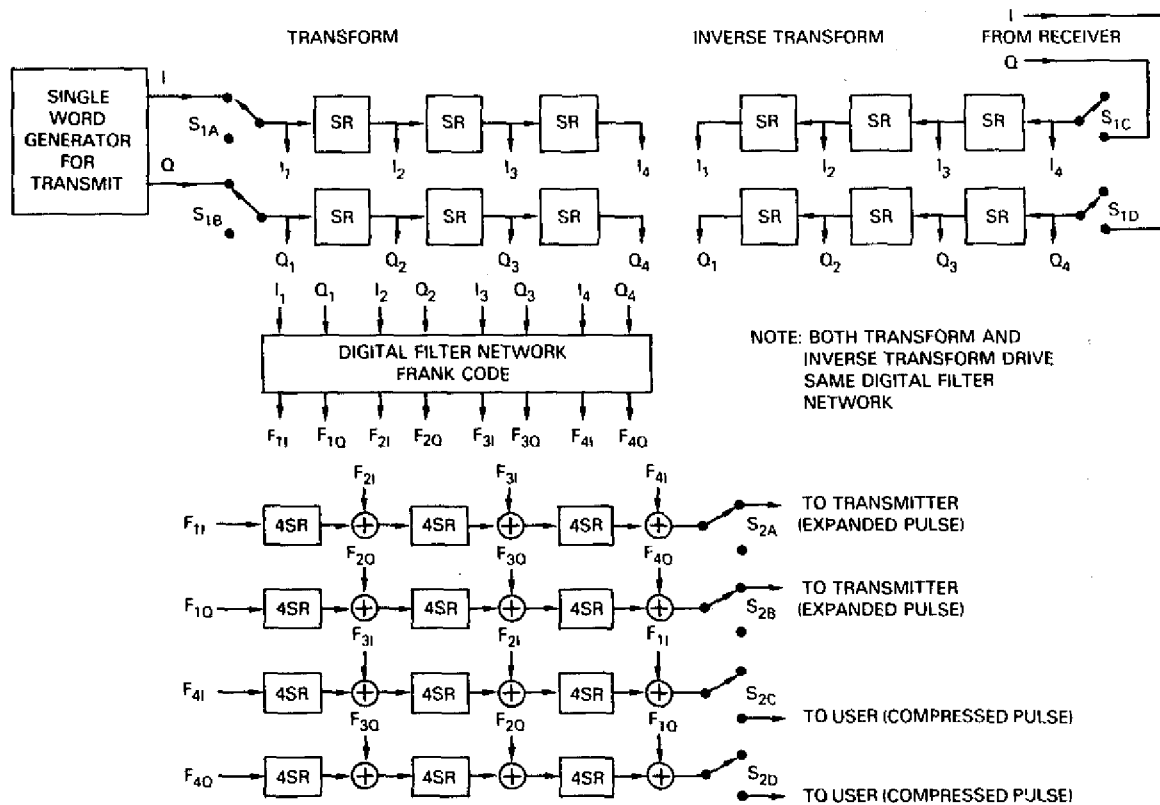


Fig. 1 — DFT pulse expander-compressor suggested by Cantrell with $N = 4$ (Frank code)

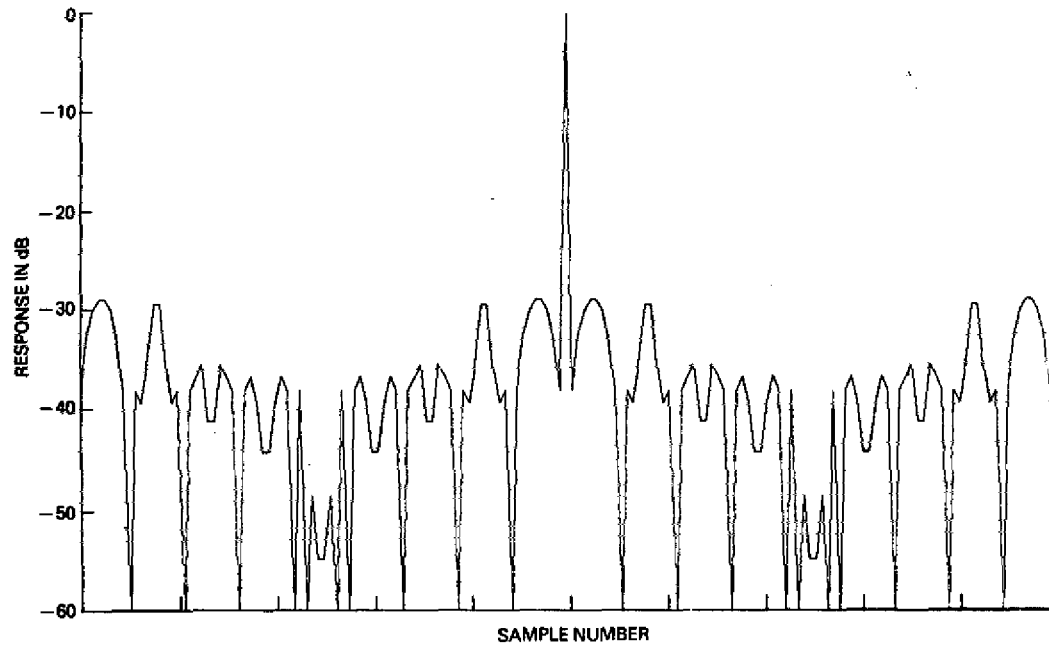


Fig. 2 — Autocorrelation function from circuit of Fig. 1 with $N = 9$

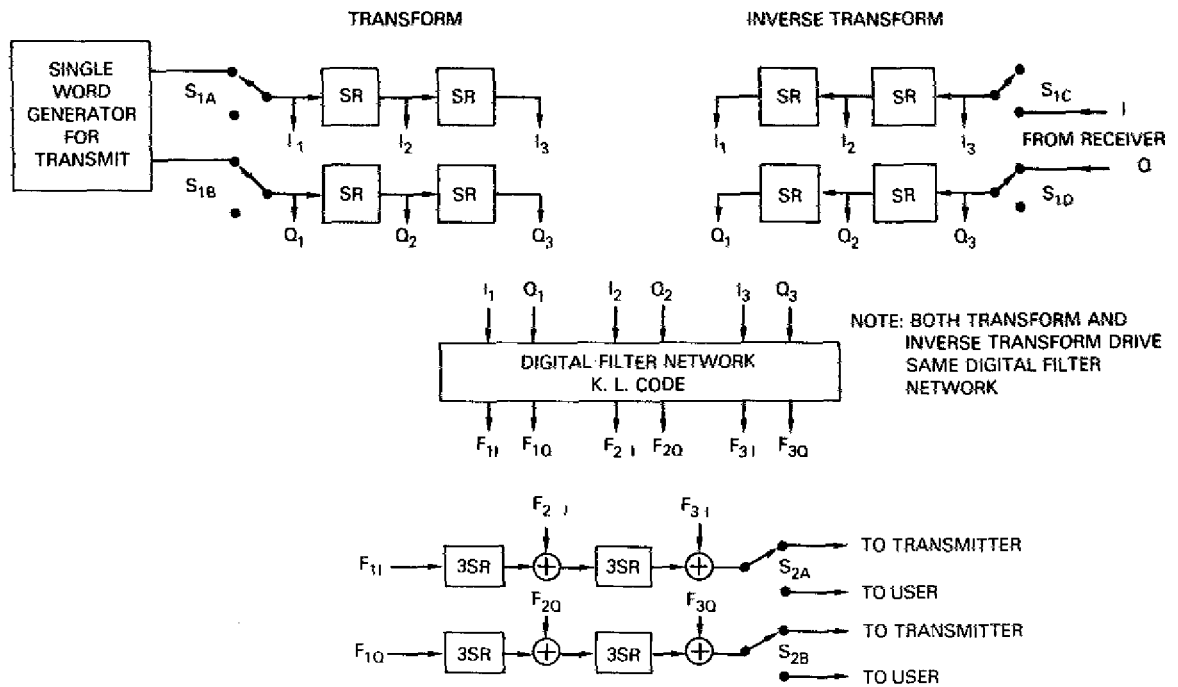


Fig. 3 — Implementation of an $N = 3$ KL code expander-compressor

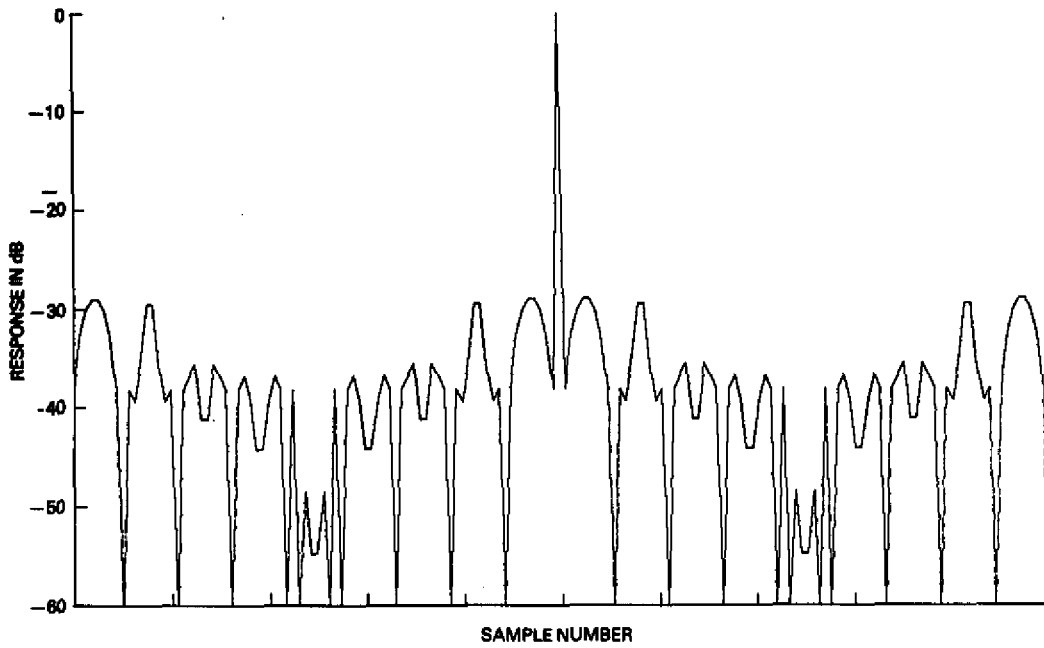


Fig. 4 — Autocorrelation function of KL code circuit of Fig. 3 with $N = 9$

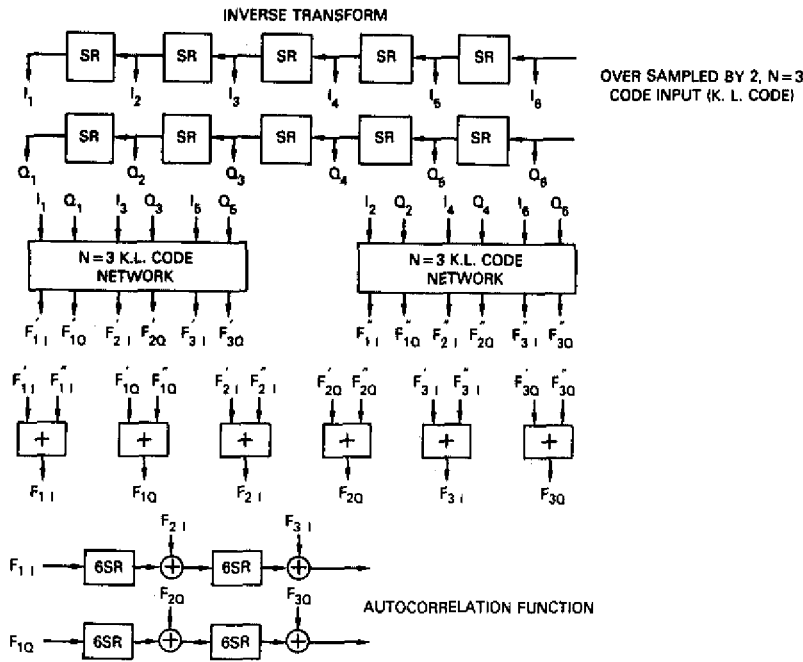


Fig. 5 — Oversampling processor KL code

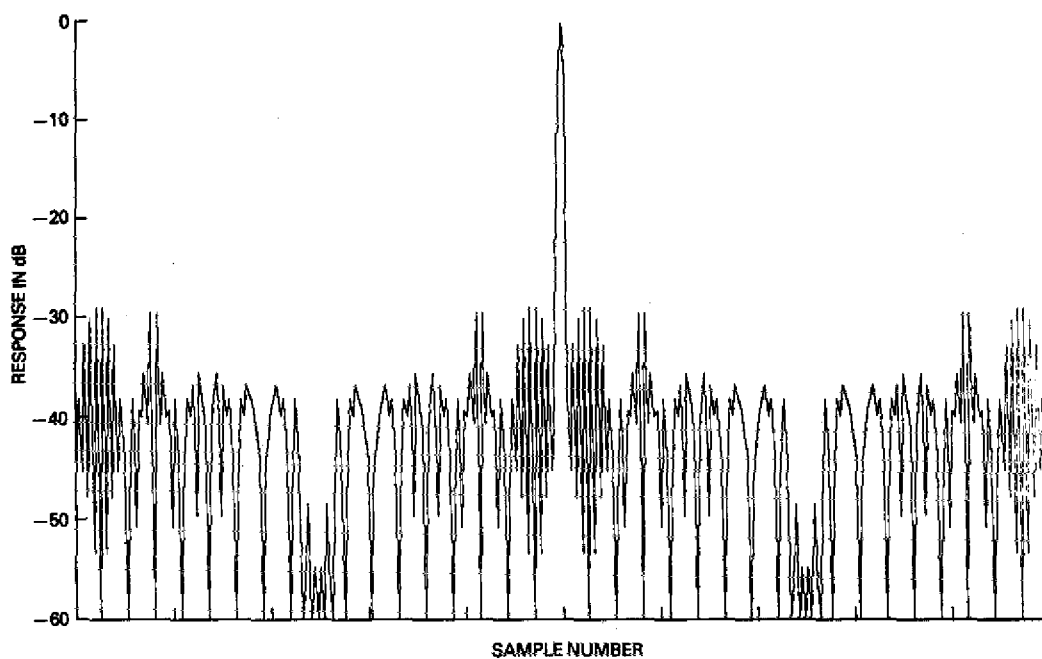


Fig. 6 — Autocorrelation function of an $N = 9$ KL code oversampled 2 to 1 and processed as illustrated in Fig. 5

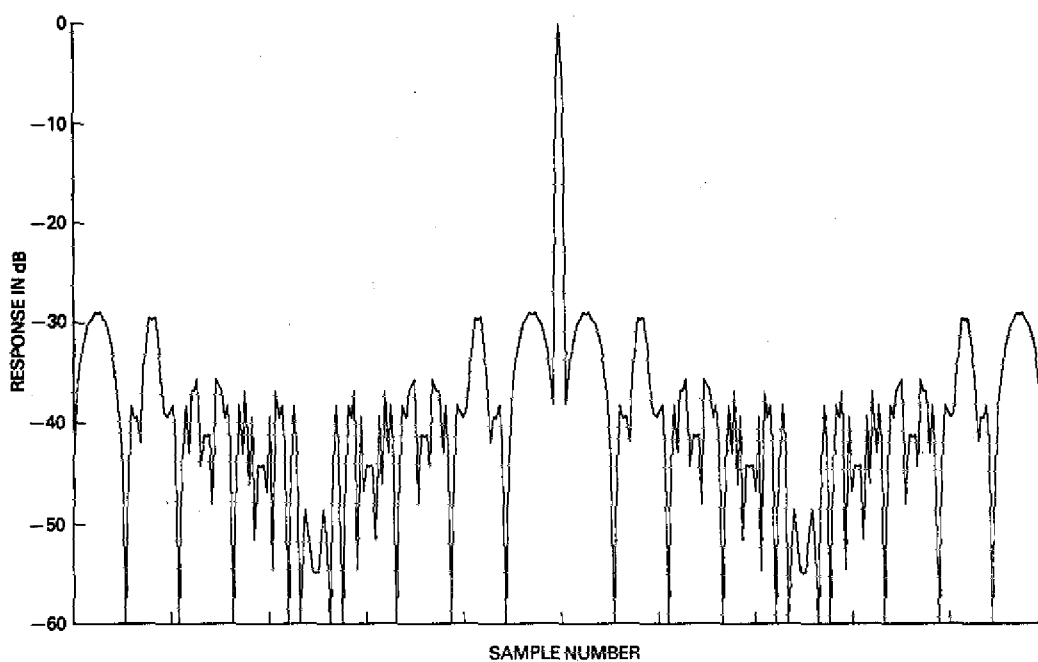


Fig. 7 — Autocorrelation function of an $N = 9$ Frank code oversampled by 2 to 1 and processed as in Fig. 5

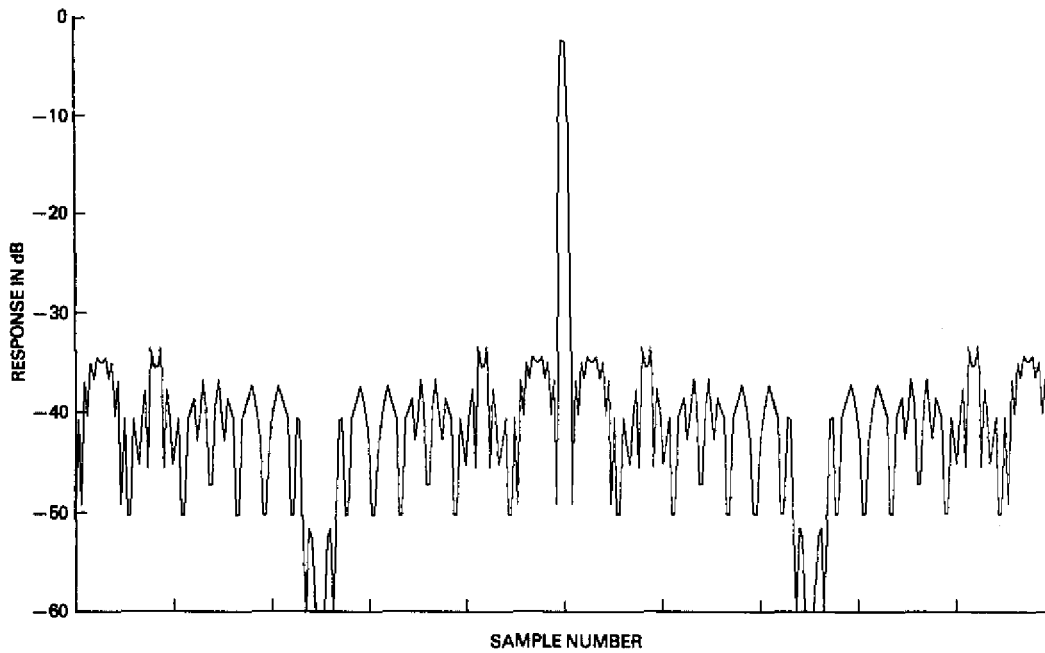


Fig. 8 — Autocorrelation function of KL code with $N = 9$ oversampled to 2 to 1 and averaged with a sliding window two sample average

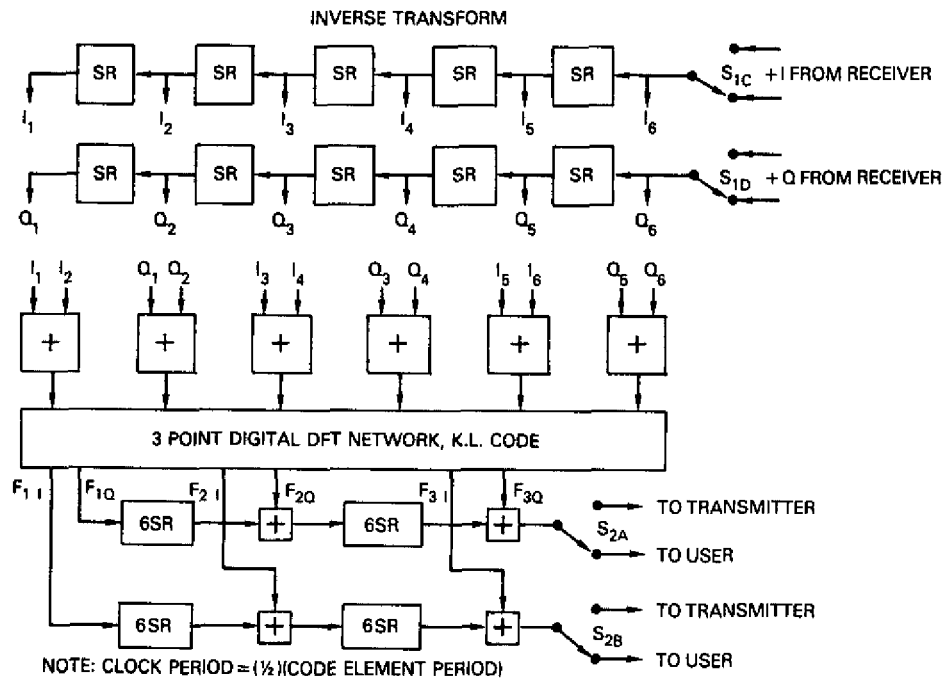


Fig. 9 — Oversampling and averaging KL code

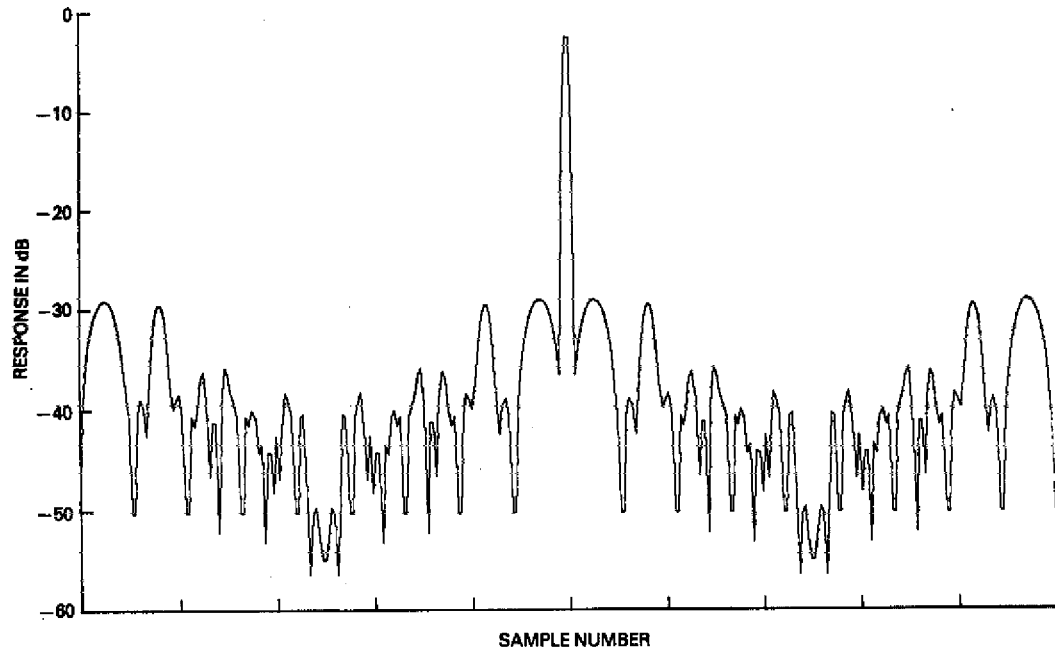


Fig. 10 — Autocorrelation function of the Frank code oversampled by 2 to 1 and averaged with a sliding window two sample average

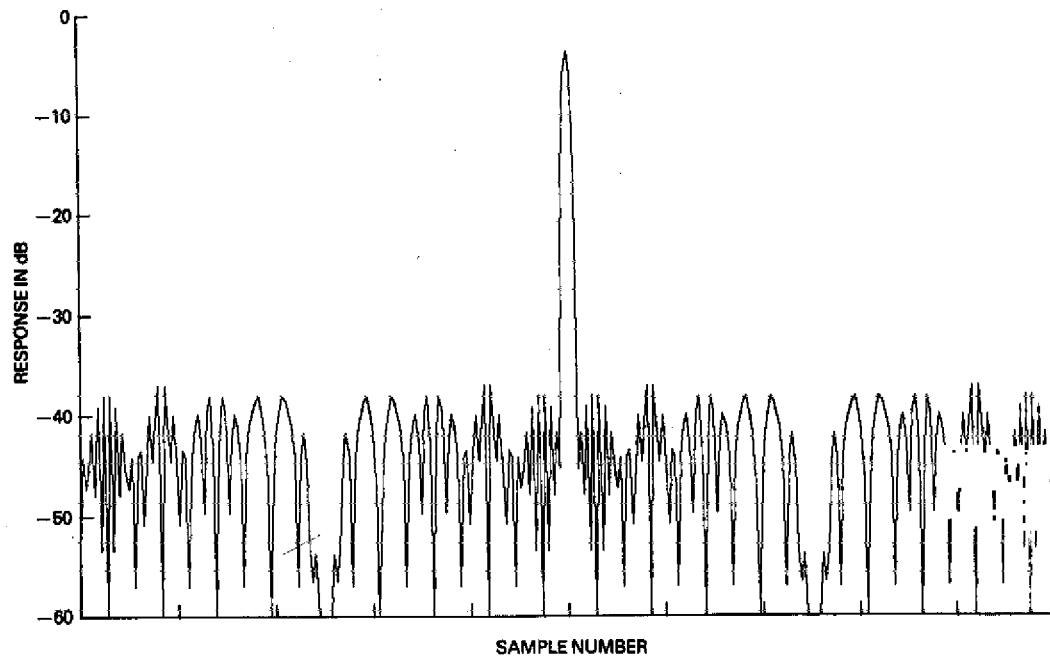


Fig. 11 — Autocorrelation function of KL code with $N = 9$ oversampled by 2 to 1 and averaged with a sliding window three sample average

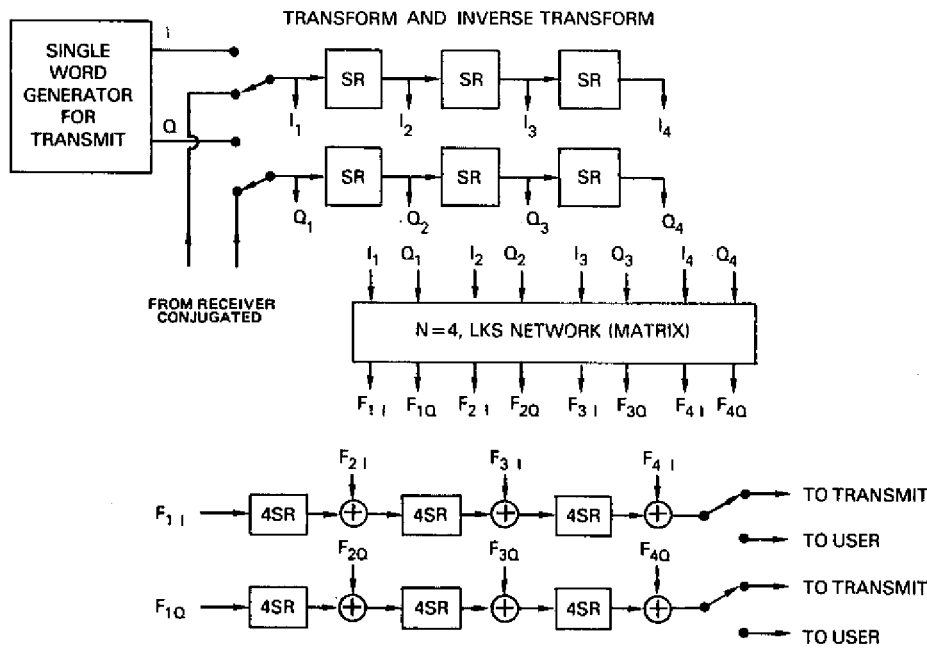


Fig. 12 — LKS code implementation with $N = 4$

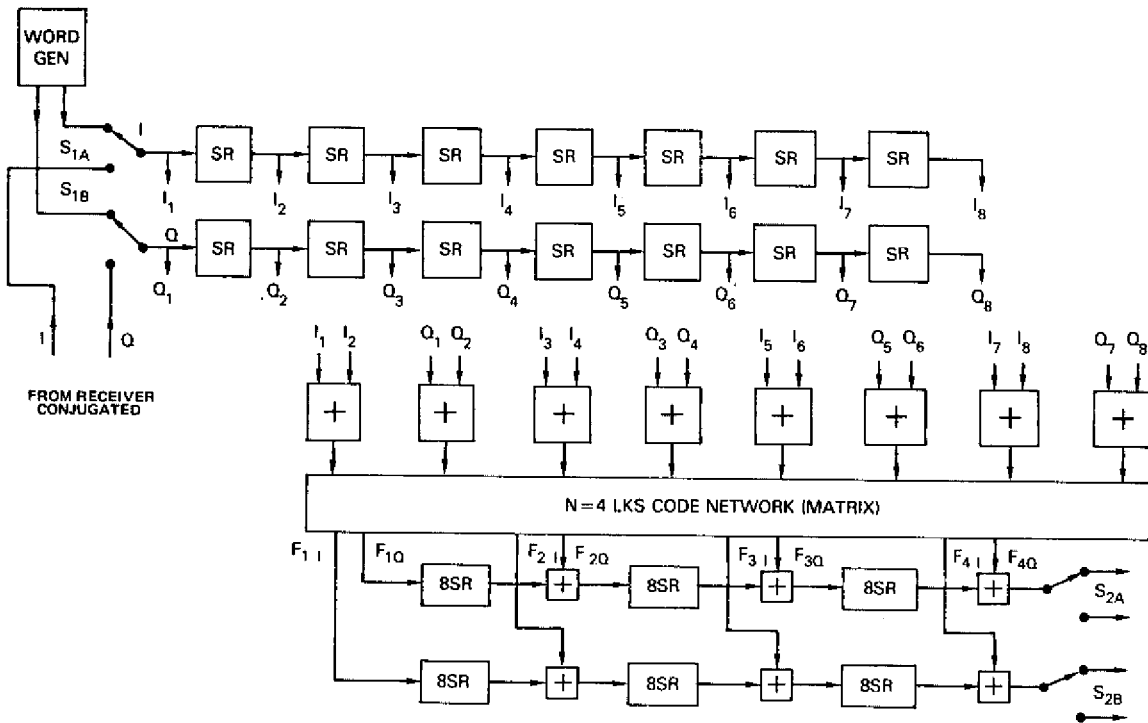


Fig. 13 — LKS code compressor illustrating oversampling by 2 and averaging by 2

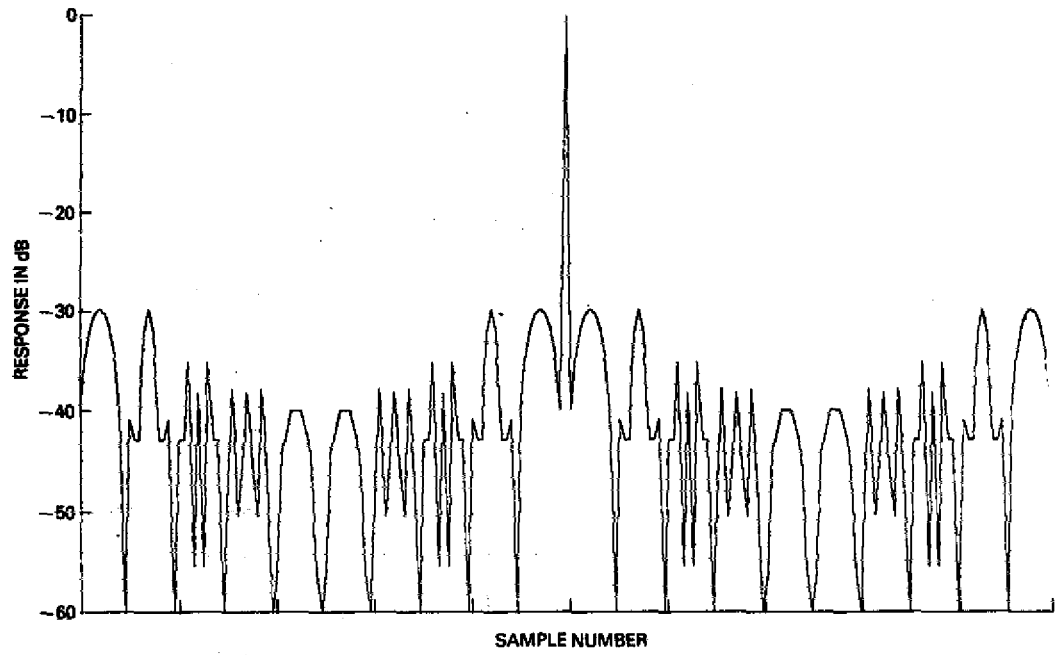


Fig. 14 — Autocorrelation function of an $N = 10$ LKS code

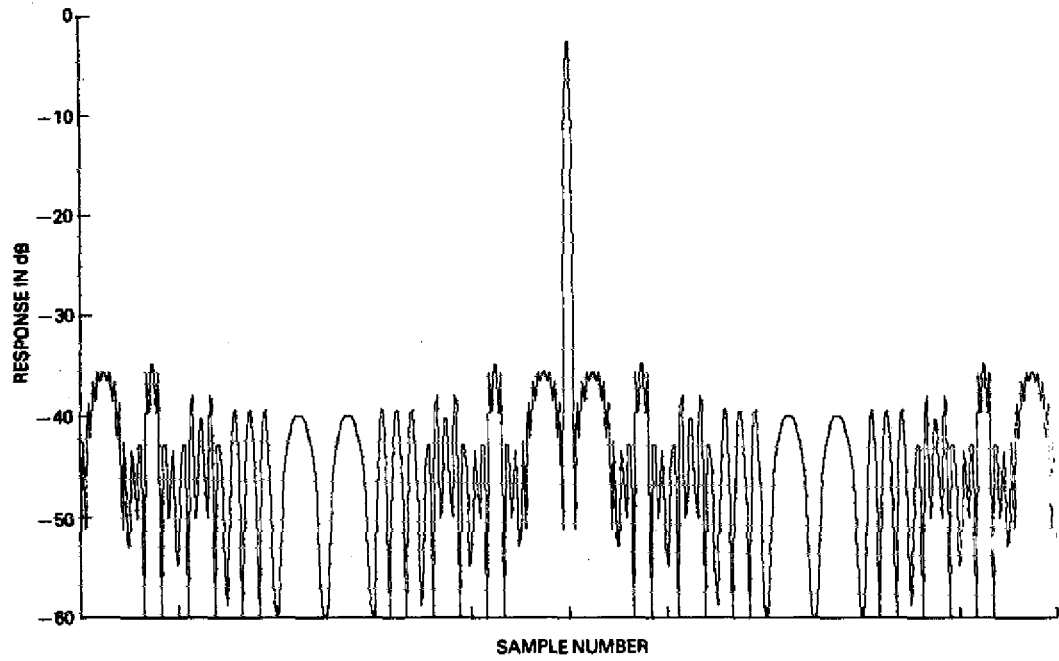


Fig. 15 — Autocorrelation function of an $N = 10$ LKS code oversampled 2 to 1 and averaged with a sliding window two sample average

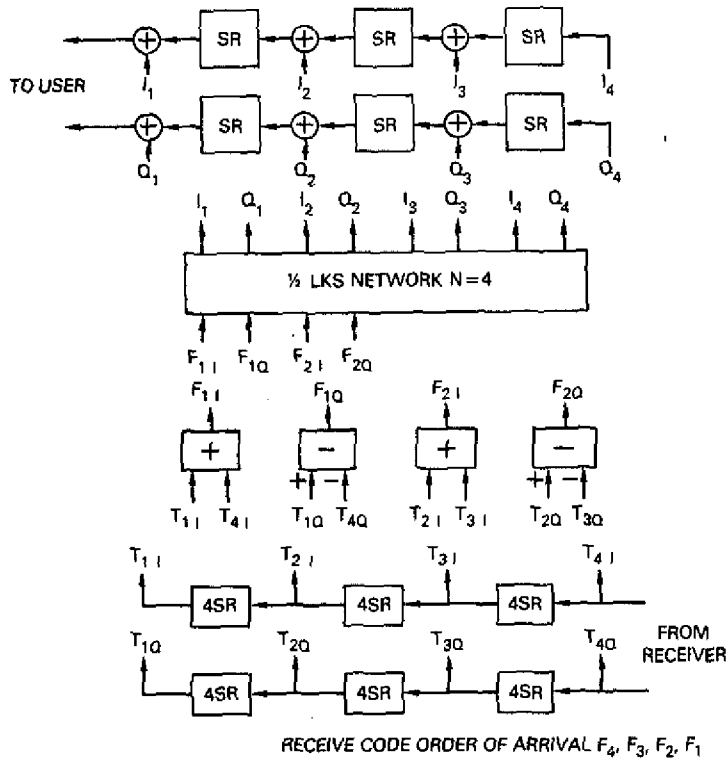


Fig. 16 — One half matrix compressor

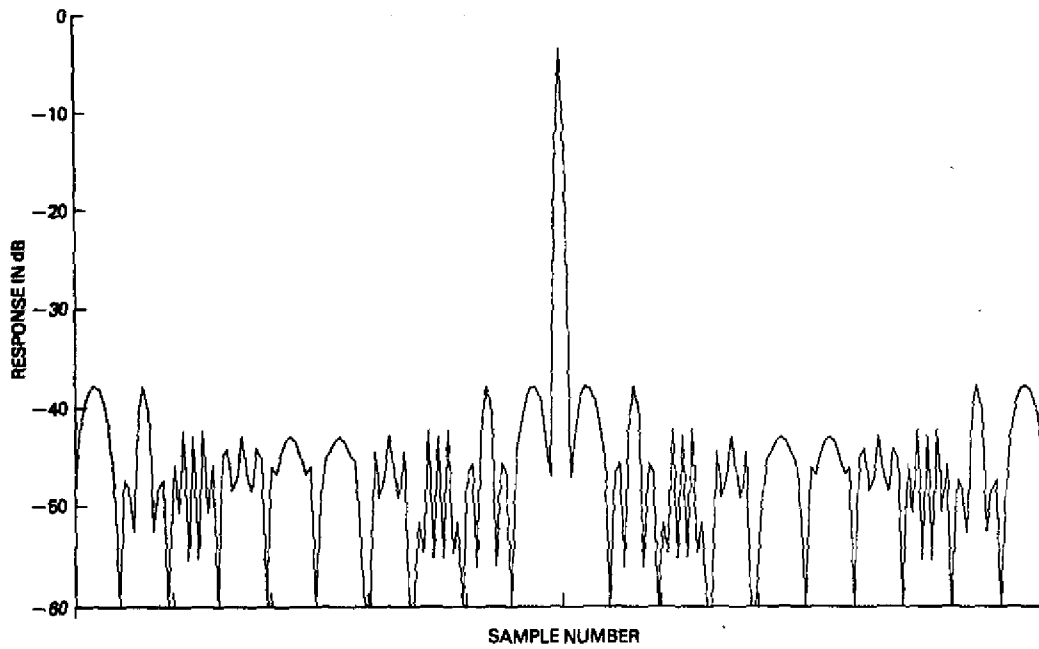


Fig. 17 — Effect of amplitude weighting, with a cosine on a pedestal of 0.4, the frequency output ports of LKS code with $N = 10$

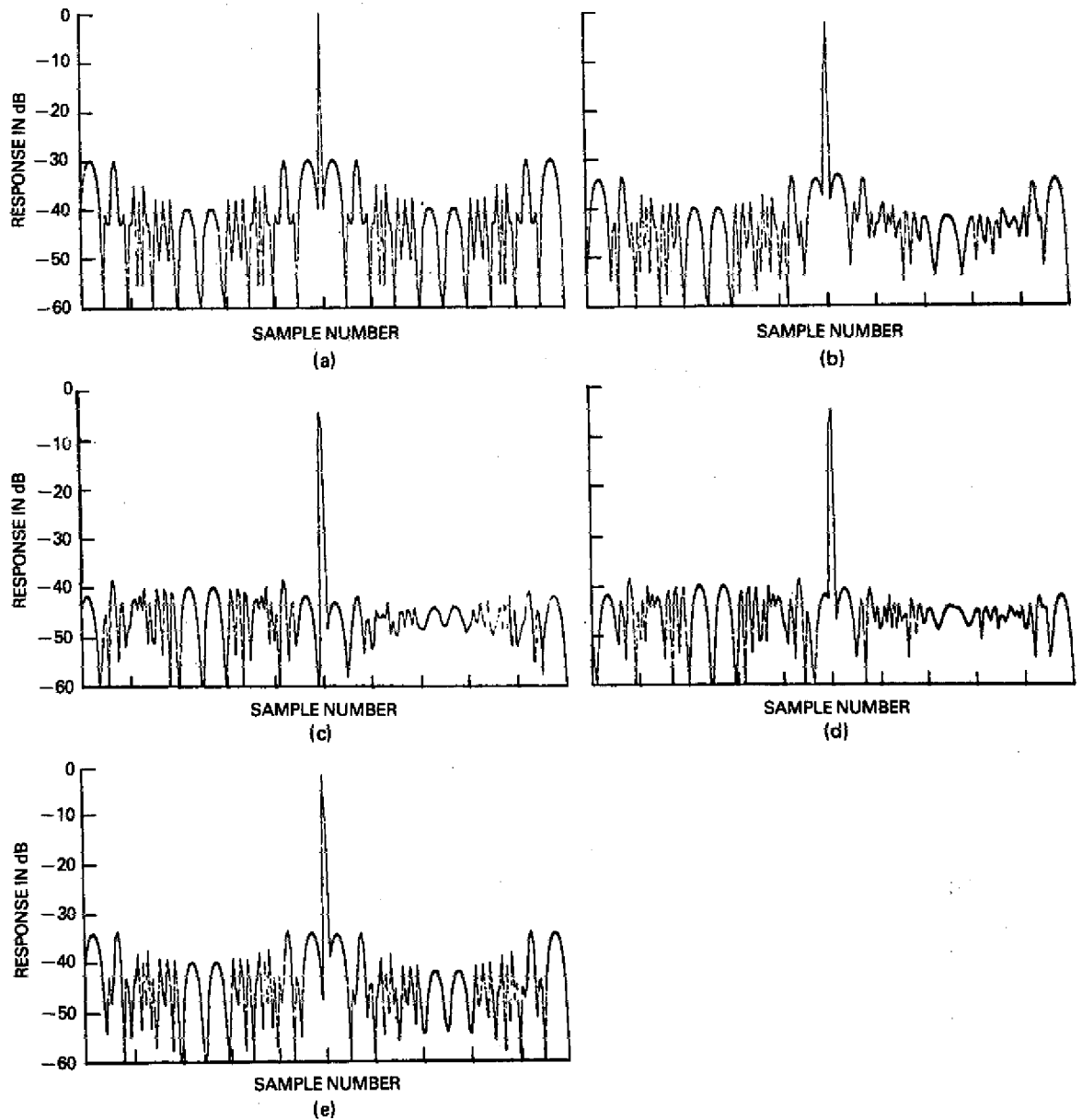


Fig. 18 — Effect of precompression bandwidth limitations on $N = 10$ LKS code with 5 sample average started (a) 5, (b) 4, (c) 3, (d) 2, and (e) 1 samples ahead of first point to be input to compressor illustrating time-of-arrival effect

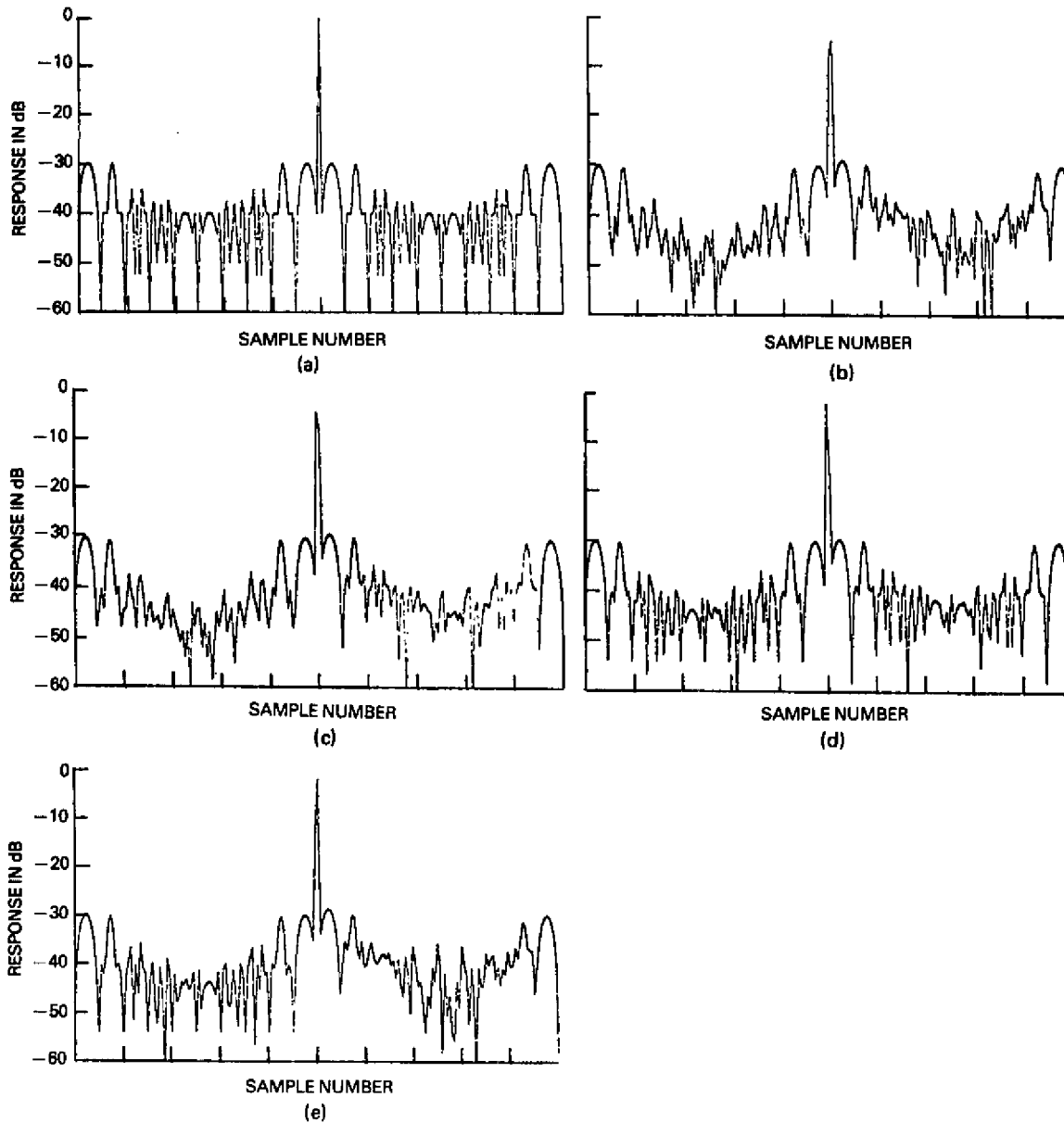


Fig. 19 — Effect of precompression bandwidth limitations on an $N = 10$ Frank code with 5-sample average started (a) 5, (b) 4, (c) 3, (d) 2, and (e) 1 samples ahead of first point to be input to compressor illustrating time of arrival effect

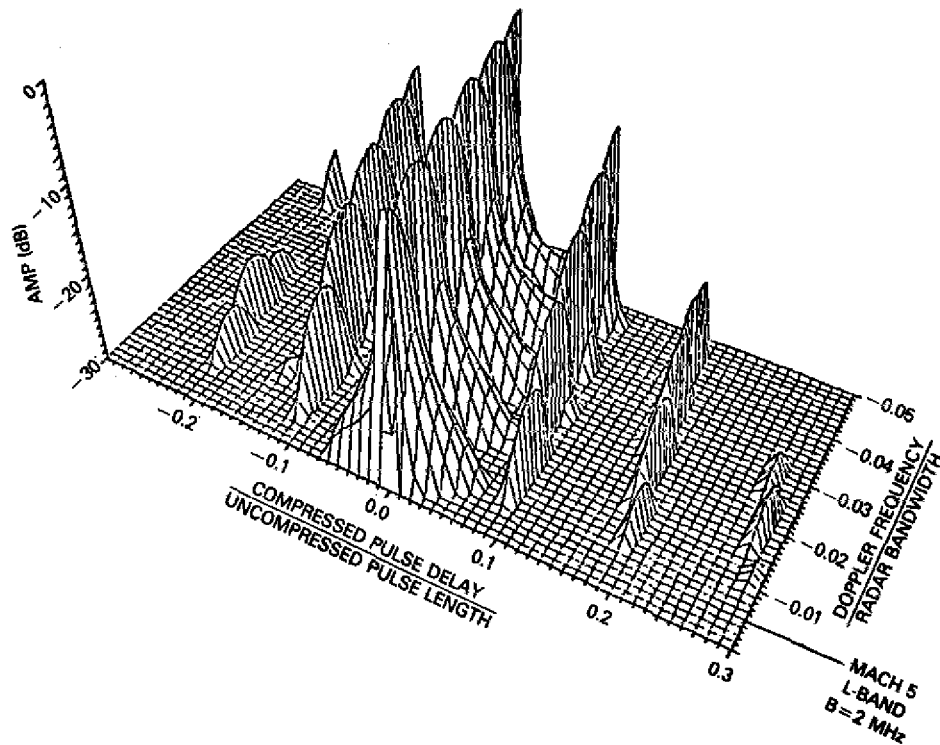


Fig. 20 — Magnified ambiguity diagram of an $N = 10$ Frank code illustrating effect of small Doppler shifts on mainlobe amplitude

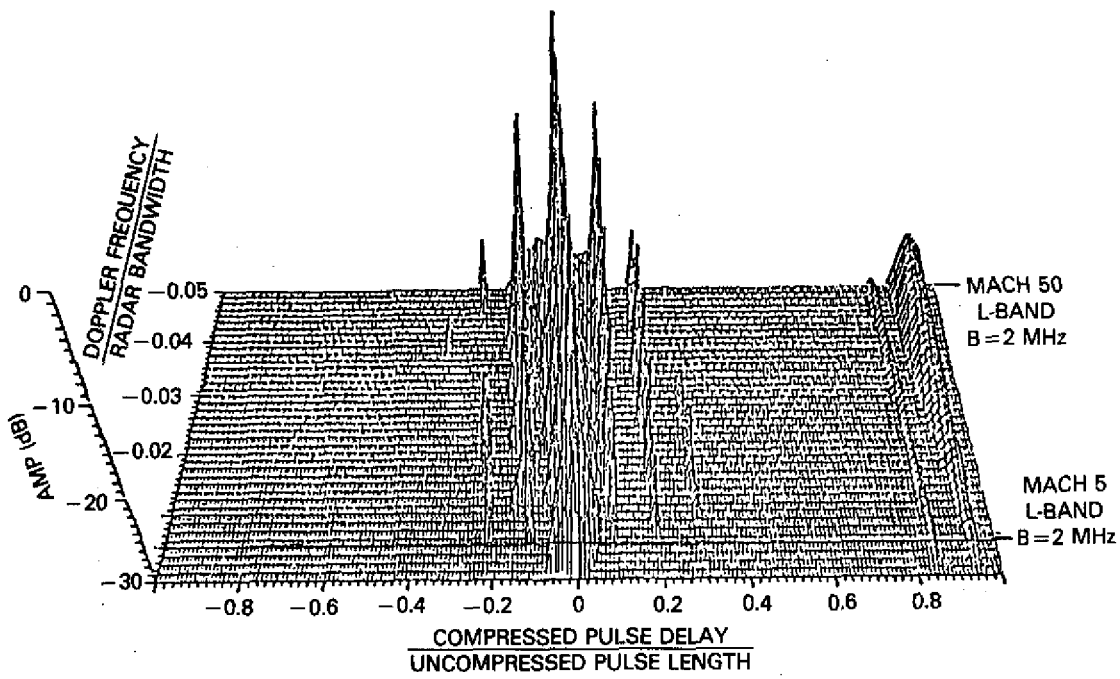


Fig. 21 — Ambiguity diagram of $N = 10$ Frank code illustrating far-out sidelobe growth with increasing Doppler shifts

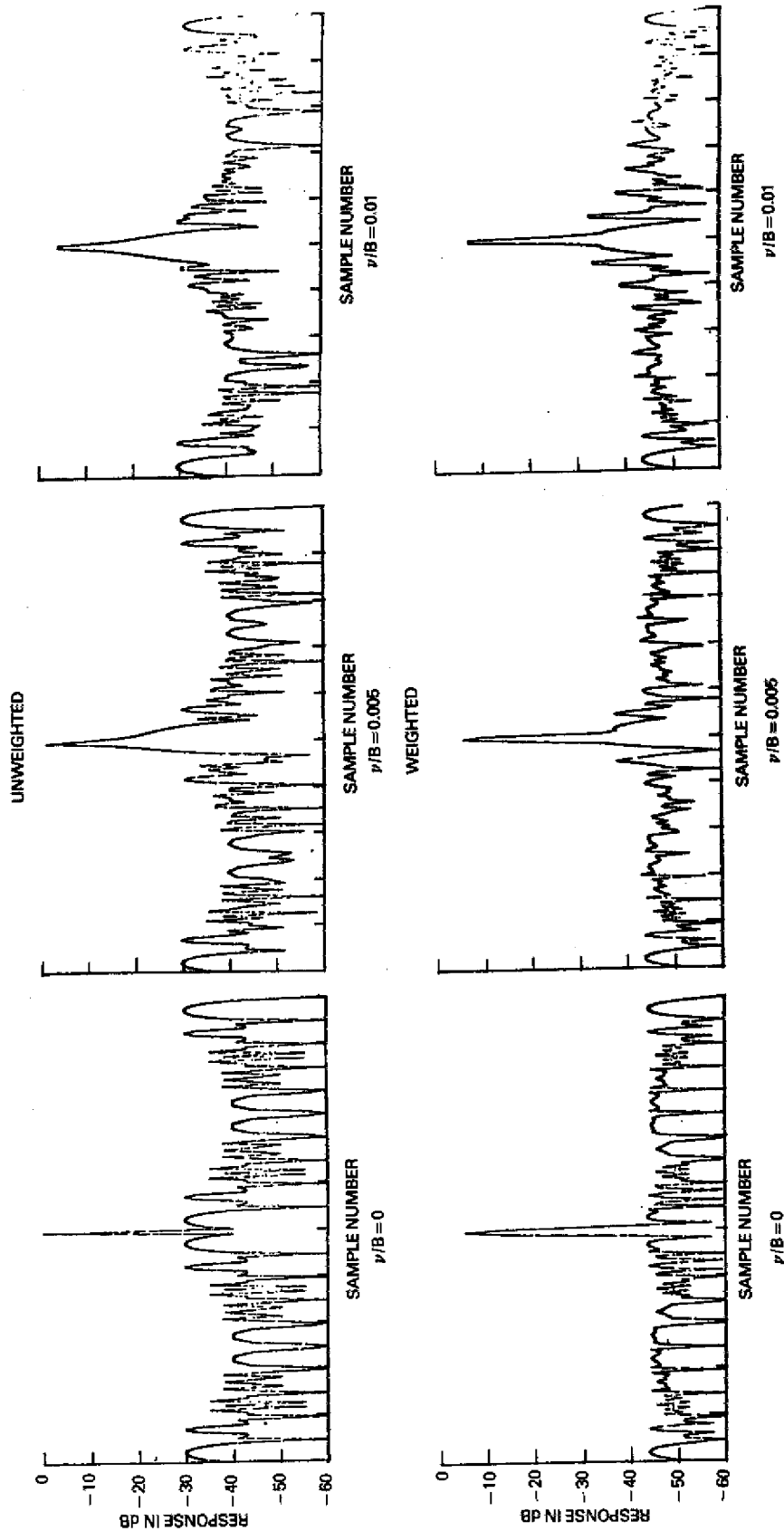


Fig. 22 — Effect of Doppler on LKS code compressor with and without amplitude weighting of frequency ports with a pedestal of 0.2

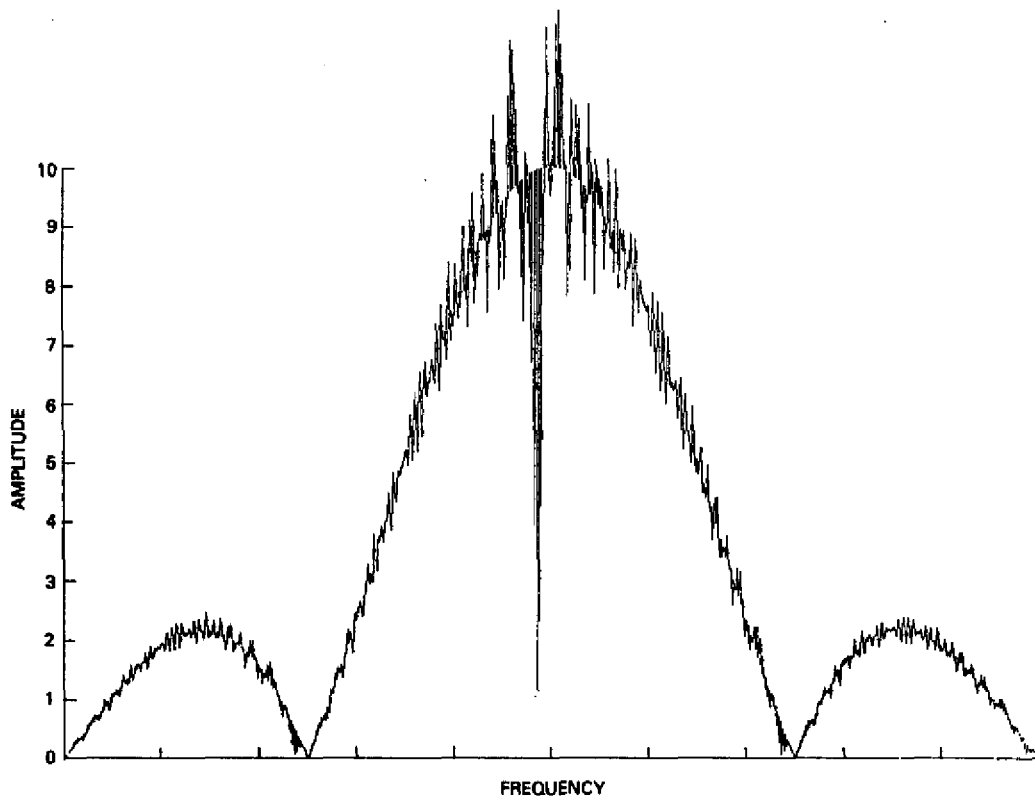


Fig. 23 — Spectrum of an $N = 10$ Frank code

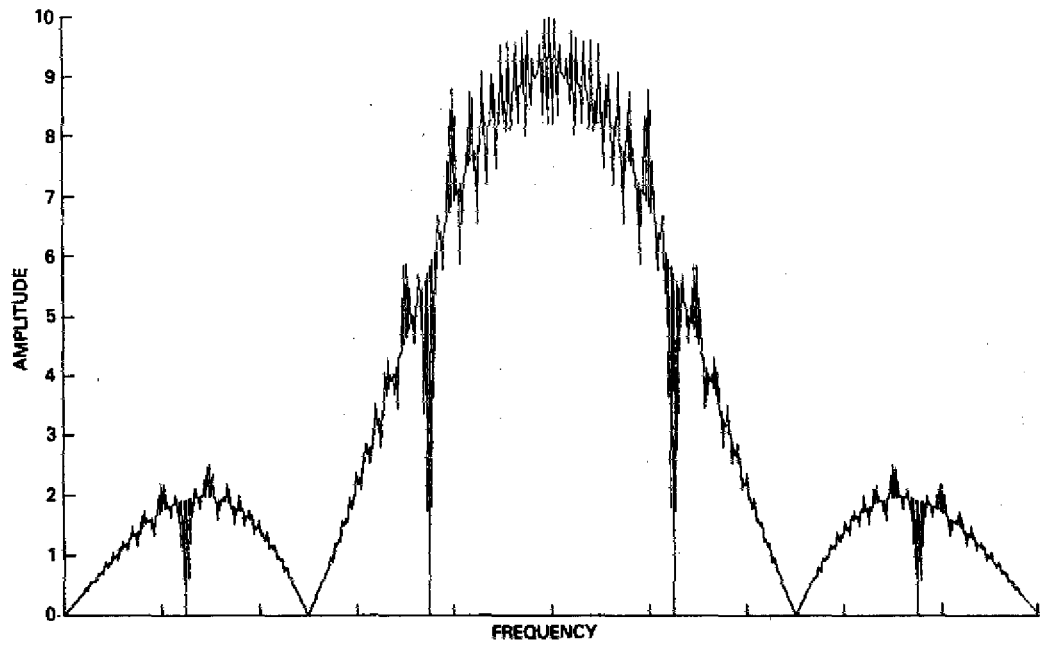


Fig. 24 - Spectrum of an $N = 10$ LKS code

CONCLUSIONS

The new codes described in this report have significant advantages over previously known codes. The new code symmetry permits digital pulse expander-compressors to be implemented with half of the normally required filter networks. In addition, the new codes can be implemented in a manner that produces lower range-time-sidelobes than any previously known code with equivalent signal-to-noise ratio loss. The latter advantage is gained by oversampling and averaging the codes at the input to the compressor. Another significant advantage of the new codes is that precompression bandwidth limiting such as would normally be found in any well-designed radar actually improves the mainlobe to sidelobe ratios obtainable with the new codes while it degrades that obtainable with the previously known Frank code.

REFERENCES

1. C.E. Cook and M. Bernfeld, "Radar Signals, An Introduction to Theory and Application," Academic Press, New York, London, 1967.
2. M.I. Skolnik, ed., "Radar Handbook," McGraw-Hill, 11-66, New York, 1970.
3. B.H. Cantrell and B.L. Lewis, Patent Application, Navy Case 61,437, "High Speed Digital Pulse Compressor," 9 Nov. 1976.
4. F.E. Nathanson, "Radar Design Principles," McGraw-Hill, New York, 1969.
5. R.L. Frank, "Polyphase Codes with Good Nonperiodic Correlation Properties," IEEE Trans. IT-9, 43-45, Jan. 1963.